

K. MAŁYSA*, S. NG**, J. CZARNECKI**, J. MASLIYAH***

THE METHOD OF DETERMINATION OF SIZES, RISE VELOCITIES AND COMPOSITION OF AGGREGATES FLOATING TO FROTH LAYER

The method of analysis of bubble-solids aggregates flow inside a flotation cell, beneath froth layer, is presented. Size, shape, rise velocity and number of the aggregates were determined using a device called the Luba tube. The experiments were carried out at 25°C in a 5.2 m diameter separation vessel used in a 100 tones per hour field pilot plant for oilsands processing. It was found that bitumen was transported to the froth layer in the form of irregular particles attached to air bubbles. A wide range of the bitumen–air aggregate sizes (from 0.13 mm to 2.84 mm) was observed with an average Feret diameter, i.e. an equivalent circular diameter of 0.68 ± 0.35 mm. Under steady state conditions the average aggregate rise velocity was 6.8 ± 1.8 cm/s with velocities varying from 3.0 to 12.6 cm/s. Mass of bitumen contained in a bitumen–air aggregate was determined on the basis of the experimental values of the aggregate size and rise velocity and the relationships describing velocity of unloaded contaminated (Model A) and clean (Model B) bubbles. It was found that mass of bitumen contained in a bubble-bitumen aggregate was of an order from 10^{-6} to 10^{-4} g depending on the aggregate dimension and the model used. The evaluated equivalent diameters of bitumen particle and air bubble making-up a bitumen–air aggregate were of a similar magnitude within ca. 0.2-1.2 mm range.

INTRODUCTION

The ultimate aim of a flotation process is to obtain high recovery of the valuable component accompanied by high selectivity of the separation. Valuable component of an ore is transported to the froth layer in the form of bubble-particle aggregates, where bubbles act as a carrier for the particles. Thus, flotation recovery for a given feed depends on the number of aggregates reporting to the froth layer, amount of the valuable component contained in the aggregates and on their rise velocity. Monitoring the aggregates flow to a froth layer in different areas of a flotation cell can be helpful for evaluation of a flotation cell performance and can provide useful information about

*Institute of Catalysis and Surface Chemistry Polish Academy of Sciences, ul. Niezapominajek 1, Cracow.

**Sincruce Research Centre, Edmonton, Canada.

***University of Alberta, Dept. Chemical & Material Engineering, Edmonton, Canada.

the processes occurring below the froth layer. A method of visualization of the bitumen–air aggregates flow inside a separation vessel has been elaborated and used for some years at Syncrude Edmonton Research Centre, Canada. Details of the apparatus and the method of analysis used in studies of mechanism of the bitumen transport in low temperature extraction process of bitumen from oilsands has been described recently (Małysa et al., 1998 a).

In this paper a method of determination of sizes, rise velocities, and composition of air-solids aggregates floating to froth layer inside a flotation cell is described. Principle, possibilities, and limitations of the method are discussed on an example of the data obtained in a study of bubble-bitumen aggregates flow inside a separation vessel. The method can be used as well to study of the aggregate flow in any flotation cell and in evaluation of its performance. Moreover, amounts of solids and air contained in aggregates floating inside a flotation cell can be calculated on a basis of differences in rise velocities of the aggregates and unloaded air bubbles. In the analysis (Małysa et al., 1998b) a relationship describing rise velocity of unloaded air bubbles of identical dimensions as an aggregate is used as a “reference state” to calculate the mass of solids contained in an aggregate. The method of analysis is illustrated by results obtained in the evaluation of mass of bitumen contained in bitumen-bubble aggregates floating inside a separation vessel for low energy bitumen extraction process, i.e. for the extraction process performed at the temperature of 25° C.

EXPERIMENTAL

Apparatus

The principle of the method is rather well-known and often used in calibration of a volumetric gas flow rate. When a cylinder filled with water is turned upside-down and the immersed in water bottom end is opened, then the water column in the cylinder can be well above the level of water in the wider container (up to a height which balances the atmospheric pressure). Bubbles and/or flotation aggregates entering via an opened end of the cylinder rise and gather at the top under the sealed end of the cylinder (see Fig.1). Using this principle, a device called the Luba tube has been designed and used to study bitumen flotation in a primary separation vessel (a flotation cell) at low energy extraction process (Małysa et al., 1998a). The principle of operation and schematic construction of the Luba tube used in the experiments are shown in Fig.1. It consisted of an aluminum circular tube of 5 cm inner diameter, a top rectangular aluminum box with three glass windows of dimensions 6×11 cm, and closing/opening mechanism. The rectangular top part of the tube can be unscrewed for cleaning the glass windows. Washers with different opening diameters can be attached to the bottom of the tube (Fig.1) to control the number of aggregates entering the tube.

A 2 cm diameter washer opening was used in the reported tests. The bottom of the tube can be opened or closed by a remote handle which controlled a cover seal over the bottom opening. Sony CCD-V101 video Hi8 Handycam, with additional lenses to increase magnification, was used to record the flow of the aggregates inside the Luba tube. A backward illumination was applied.

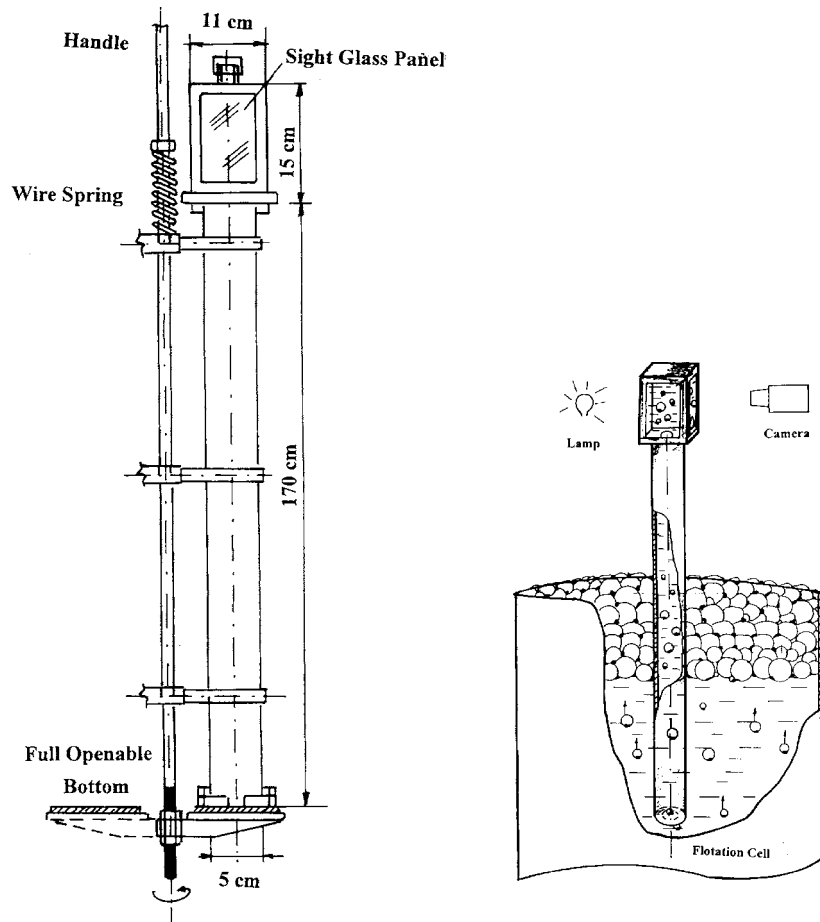


Fig. 1. A principle of operation and a schematic drawing of the Luba tube apparatus
Rys. 1. Zasada działania i schematyczny rysunek aparatu Luby

The experiments were carried out in a 5.2 m diameter flotation cell (Primary Separation Vessel-PSV) used in processing of oilsand ore containing 8.8% bitumen and 85% solids. The locked Luba tube was immersed 70 cm into the PSV, i.e. its bottom opening was located 70 cm below the top of the froth layer. After opening the bottom entrance the flotation aggregates entered the tube and their flow was recorded via glass windows of the rectangular top part of the tube. Measurements were carried

out at 3 radial locations of the PSV; 0.9 m (location 1), 1.6 m (location 2), and 2.3 m (location 3) from the PSV centre.

Method of analysis

The flux of the aggregates to the froth layer was determined by counting the number of aggregates on every 25th frame of the recordings. Time span of 25 frames was arbitrary chosen to be long enough to prevent multiple counting of any of the aggregates. Frame grabber installed under Windows 3.11 was used to grab and digitize the chosen frames of the recordings. SigmaScan Pro automated image analysis software (SigmaScanPro, 1995) was used to determine the shape, size and rise velocity of the aggregates. To determine the afore-mentioned parameters, sequences of few frames were grabbed and digitized for various observation times. Identical procedure was always applied in image analysis of the grabbed frames to determine area, Feret diameter, and shape factor of the aggregates. Feret diameter (d_F), or the equivalent circular diameter (Russ, 1995) is the diameter of a fictitious circular object that has the same area as the irregular object being measured. Shape factor (SF) was used as a quantitative description of non-sphericity of the aggregates. A perfect circle has a shape factor of unity, and a line has a shape factor approaching zero.

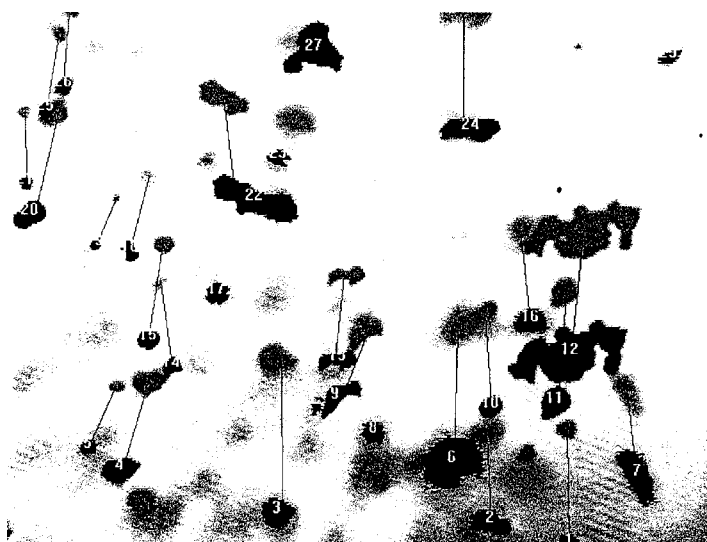


Fig. 2. An example of frame illustrating changes in aggregate positions within time interval of $\Delta t = 1/30$ s.

Rys. 2. Przykładowa klatka video pokazująca zmiany pozycji agregatów w czasie $\Delta t = 1/30$ s

To determine an aggregate rise velocity, frame “ $i + 1$ ” was added to frame “ i ” after processing every frame using the SigmaScan Pro automated image analysis software. As a result of this addition two subsequent positions of an aggregate within a time interval of $\Delta t = 1/30$ s were obtained on frame “ i ”, and the distance between two positions of every aggregate was measured. Figure 2 shows an example of such frame “ i ” and the distance measured between subsequent positions of every aggregate present on frame “ $i + 1$ ”. The velocity U of an aggregate was calculated as:

$$U = \frac{\sqrt{(x_2 - x_1)^2 + (y_2 - y_1)^2}}{\Delta t} \quad (1)$$

where (x_2, y_2) and (x_1, y_1) are coordinates of an aggregate on frame “ $i + 1$ ” and “ i ”, respectively, and Δt is the time interval between the frames.

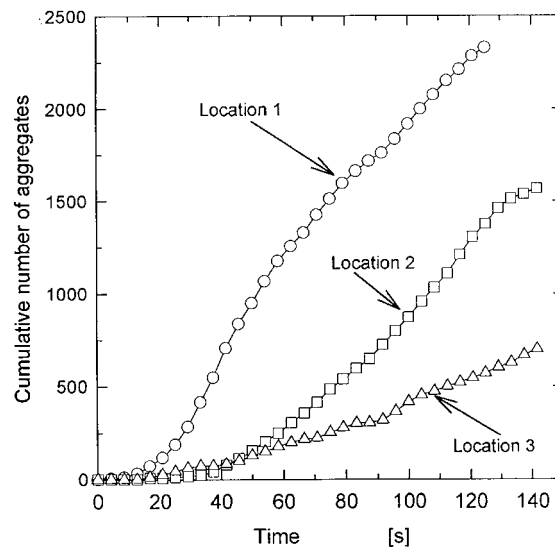


Fig. 3. Cumulative numbers of aggregates counted as a function of observation time for three different radial locations at the separation vessel
Rys. 3. Sumaryczna liczba zliczanych agregatów w funkcji czasu obserwacji dla trzech różnych radialnych pozycji w komorze flotacyjnej

RESULTS AND DISCUSSION

Flux of the aggregates to froth

Figure 3 presents the cumulative number of the aggregates floating to the froth layer as a function of the observation time for three different radial locations in the

PSV. Here, the observation time is the time elapsed from the moment when the first bubble was recorded. It is seen that the cumulative number of the aggregates floating to the froth layer was strongly depended on the radial location in the PSV. The highest counted number of the aggregates reporting to the froth layer was found at location 1, i.e. 0.9 m from the center of the PSV, and the lowest value was observed at location 3, i.e. at a point 2.3 m from the PSV center and only 0.3 m from the PSV wall. For example for the observation time $t = 120$ s the ratio of the number of aggregates at the location 1 to that at the location 2 was 1.7, while for the locations 1 and 3 that ratio was 4.1.

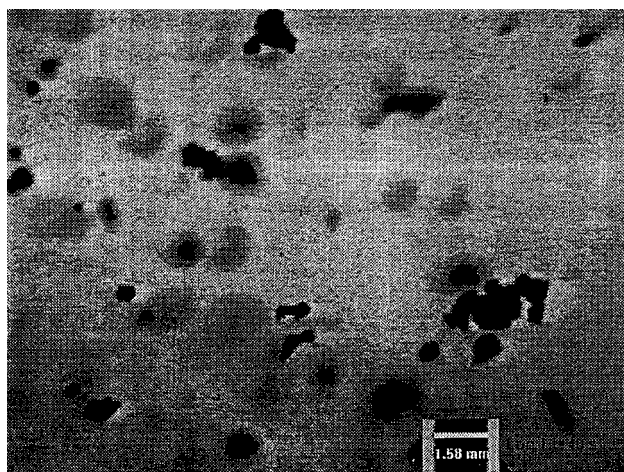


Fig. 4. Bitumen–air aggregates at location 1 and time of observation 40.4 s
Rys. 4. Agregaty bitumin–bąńka powietrza w lokalizacji 1 i po czasie obserwacji 40,4 s

The results shown in Fig. 3 indicate that the performance of the tested separation vessel was not the best one possible because recovery differed significantly in various areas of the vessel. The majority of bitumen reported to the froth layer was in the vicinity of location 1. This uneven performance of the separation vessel was most probably caused by an uneven feed distribution over the vessel area (the feed was supplied to the central area of the PSV). An independent froth production rate measurements (Malysa et al., 1998a), hereafter called macroscopic measurements, showed that the ratio of froth production rate at location 1 relative to location 2 was 1.9, and location 1 relative to location 3 was 4.1. Thus, these results are in good agreement with the Luba tube measurements and confirm the dependence of the froth production on radial location in the vessel.

Shape and size of the aggregates

Shape and size of the bitumen–air aggregates found inside the separation vessel are shown in Fig. 4 presenting a frame grabbed from the video recording at location 1

for time of observation $t = 40.4$ s. An image of a rod of 1.58 mm diameter was inserted into the frame shown in Fig. 4 to show the absolute dimensions of the aggregates. Two important features can be observed immediately: i) the overwhelming majority of the aggregates had irregular, non-spherical shapes, and ii) a wide range of aggregate size is present.

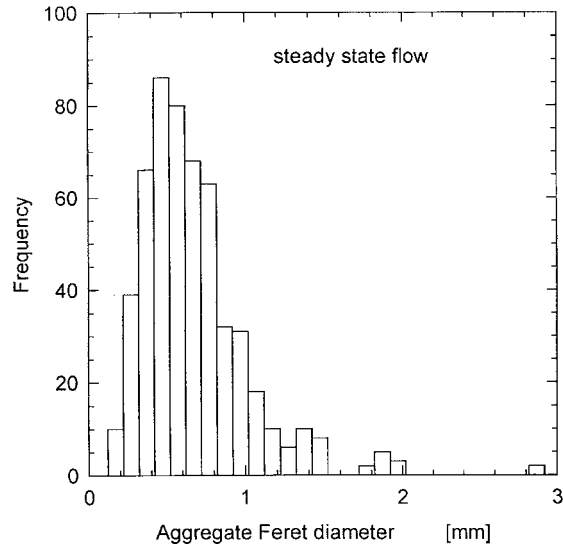


Fig. 5. Histogram of aggregate Feret diameters under steady state flow conditions
 Rys. 5. Histogram średnic Fereta agregatów przy przepływie w stanie stacjonarym

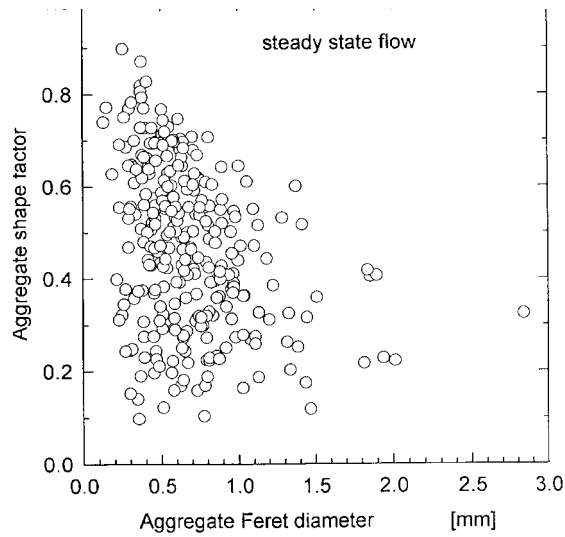


Fig. 6. Aggregate shape factor as a function of the Feret diameter
 Rys. 6. Parametr kształtu agregatów w funkcji ich średnicy Fereta

Figure 5 shows the distribution of the aggregate size floating to froth layer in location 1. The histogram presents values of the Feret diameter measured for aggregates on various frames within observation period of 15–40 s. A wide range of the aggregate size from 0.13 to 2.84 mm was found but the majority of the aggregates had Feret diameters from 0.4 to 0.8 mm (see Fig. 5). The average value of the Feret diameter was found to be 0.68 ± 0.35 mm.

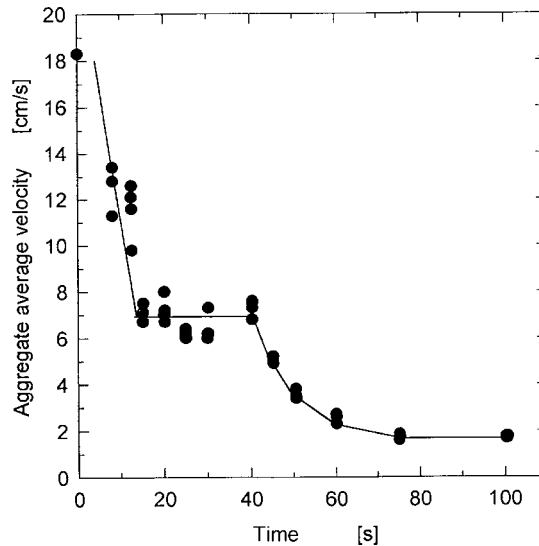


Fig. 7. Aggregate average velocity as a function of the observation time
 Fig. 7. Średnia prędkość agregatów w funkcji czasu obserwacji

Figure 6 shows the shape factor values versus the aggregate dimensions and illustrates high fluctuations in the aggregates shape. The aggregate shape factor, as shown in Fig. 6, varied from 0.1 to 0.9, i.e. fluctuated practically over the whole range of the shape factor values (shape factor can vary from 0 to 1), particularly, for the case of the smallest aggregates (Feret diameter of an order 0.2–0.5 mm). On the other hand a tendency for larger aggregates to have more irregular shape can be observed. The average value of the aggregate shape factor was 0.47 ± 0.18 , indicating a very high degree of non-sphericity.

Rise velocity of the aggregates

The average aggregate rise velocity was obtained by measuring rise velocity for every aggregate present on frames “*i*” and “*i* + 1”, or “*i*” and “*i*+2” and then their

mean value was calculated. Figure 7 presents the aggregate average rise velocity as a function of the observation time for location 1 in the separation vessel. It is seen from Fig. 7 that initially, the average aggregate rise velocity decreases rapidly with observation time. It reaches a plateau value of about 7 cm/s, for the observation time period of 15–40 s, and at longer observation times it decreases further down to 1.7 cm/s. The origin of the time axis of Fig. 7 is related to the “sampling” procedure used in the experiments.

The distance from the tube opening to the point of observation was ca. 165 cm. Thus, the aggregates needed some time to reach the point of observation after the tube was opened and the time lapse depended on the aggregate velocity. As a result of the wide spectrum of aggregate velocities, and long distance from the tube entrance to the point of observation, separation of aggregates, according to their individual velocities, took place. The fastest aggregates reached the area of observation first. With prolonged observation time, the slower aggregates reached the point of observation as well. This led to the emergence of a steady state flow period. When the tube was closed the source of the aggregate flow ceased and the observed aggregate average velocity started to decrease due to the lack of the whole spectrum of aggregate velocities. Here again the fastest aggregates, contained inside the tube, were the first to pass through the observation area and with prolonged time of observation there were only slower and slower aggregates to be recorded. Therefore, the observed aggregate average velocity started to decrease after closing the Luba tube.

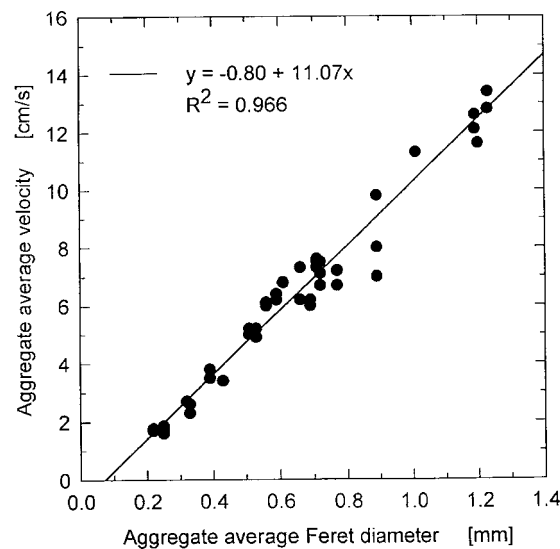


Fig. 8. Aggregate average velocity as a function of the average Feret diameter
Rys. 8. Średnia prędkość agregatów w funkcji wartości średniej średnicy Fereta

As described above, the time of observation was denoted as the time elapsed from the moment the first bubble was recorded to pass through the observation field. It was found that the velocity of the “fastest aggregate” was 18.3 cm/s (see Fig.7). It means that the real moment of the tube opening was earlier by 9 s ($165 \text{ cm}/18.3 \text{ cm s}^{-1}$). It is also worth to point out that the planned period of the Luba tube to be opened was 30 s and fairly constant aggregate average velocity (a plateau on the velocity vs. time dependence in Fig. 7) was found for the observation time from 15 to 40 s, i.e. for the time period of 25 s. Taking into account that the Luba tube opening mechanism was operated manually the agreement is remarkably good.

Figure 8 presents a correlation between the aggregate average velocity and Feret diameter. Values of the average Feret diameter were determined in a similar manner as for the aggregate average velocity, i.e. on a given frame, the Feret diameter of every aggregate present was measured and then the mean value was calculated. Figure 8 shows that the experimental data of aggregate velocity are linearly correlated with the Feret diameter. The larger aggregates had higher velocity, thus leading to an increased bitumen transport to the froth layer. A higher rise velocity means that the aggregate contained more air. This is in agreement with the observation that the largest aggregates consisted of a few air bubbles interconnected by a bitumen entity.

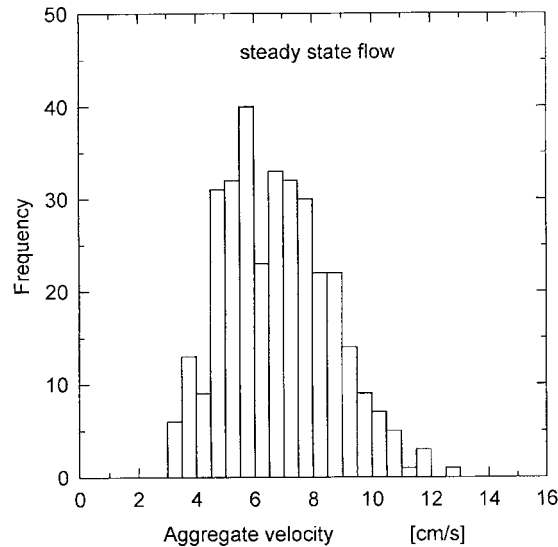


Fig. 9. Histogram of the aggregate velocities under steady state flow conditions
Rys. 9. Histogram prędkości agregatów przy przepływie w stanie stacjonarym

Figure 9 presents a velocity histogram of the velocities of individual aggregates under the steady state flow conditions. A wide range of the aggregate velocities from 3 to 12.6 cm/s was measured. However, the majority of aggregates floated with a velocity ranging from about 5 to 9 cm/s. The average aggregate rise velocity under steady state flow conditions was found to be $6.8 \pm 1.8 \text{ cm/s}$, and this value can be considered as one of the

most characteristic parameter describing bitumen–air aggregate flow in the separation vessel.

Mass of solids in the aggregates

Any bubble–solids aggregate floating to the froth layer consists of an air bubble and attached grain or a few grains. Gas bubble is a carrier transporting the attached material which generally has higher density than a continuous phase. Thus, the aggregate apparent density ρ_{aggr} should be larger than air density ρ_{air} and smaller than density of the continuous medium. The total mass of any aggregate M_{aggr} is a sum of the mass of air M_{air} and the mass of solids M_{sd} contained in the aggregate, i.e:

$$M_{\text{aggr}} = M_{\text{air}} + M_{\text{sd}} \quad (2)$$

Solids attached to an air bubble can show all variety of shapes. Similarly air bubbles can be deformed to different degree depending on their dimensions and amount of solids attached to them. The only simple way of description their shape is to use their equivalent spherical diameter, i.e. the diameter of a fictitious spherical object which would have the same volume as the irregular object being considered. Using this notion a mass of the aggregate can be expressed as:

$$M_{\text{aggr}} = \frac{\pi d_{\text{aggr}}^3 \rho_{\text{aggr}}}{6} \quad (3)$$

where d_{aggr} is the aggregate equivalent spherical diameter. Similarly

$$M_{\text{air}} = \frac{\pi d_{\text{air}}^3 \rho_{\text{air}}}{6} \quad (4)$$

and

$$M_{\text{sd}} = \frac{\pi \rho_{\text{sd}} (d_{\text{aggr}}^3 - d_{\text{air}}^3)}{6} \quad (5)$$

where ρ_{sd} is the solids density and d_{air} is the equivalent spherical diameter of air contained in the aggregate. Using Eqs. (2)–(5) the bubble diameter d_{air} can be expressed as:

$$d_{\text{air}} = d_{\text{aggr}} \left(\frac{\rho_{\text{sd}} - \rho_{\text{aggr}}}{\rho_{\text{sd}} - \rho_{\text{air}}} \right)^{1/3} \quad (6)$$

and the mass of solids M_{sd} as:

$$M_{sd} = \frac{\pi}{6} \rho_{sd} d_{aggr}^3 \left(1 - \frac{\rho_{sd} - \rho_{aggr}}{\rho_{sd} - \rho_{air}} \right) \quad (7)$$

Solids density is normally easily available and thus, the aggregate diameter and its apparent density are the only additional data needed to calculate from Eq. (7) the mass of solids contained in an aggregate. Taking into account that normally $\rho_{air} \ll \rho_{sd}$

$$M_{sd} = \frac{\pi}{6} d_{aggr}^3 \rho_{aggr} \quad (8)$$

It is worth to point out here that M_{sd} in Eq. (8) is independent of the solids density. Thus, in the case when solids density is not available then this approximate relationship can be used to evaluate the mass of solids in an aggregate.

The apparent density of an aggregate can be found by calculation density difference which caused lowering velocity of unloaded air bubble to the measured velocity of a bubble–solids aggregate of identical dimension. Relationship describing velocity of unloaded air bubble is the “reference state” needed to determine the mass of solids contained in the aggregate. Thus, values of the quantities determined will depend on a choice of the “reference state”.

According to Yoon and Luttrell (1989) the range of Reynolds numbers encountered for the size of bubbles typically employed during flotation fall into a range of 0.2 to 100. There is no available a general relationship describing bubble velocity for all flow conditions encountered in a flotation cell. Thus, empirical relationships describing i) motion of unloaded contaminated bubbles (Clift et al., 1978), and ii) unloaded clean bubbles, i.e. without any surface active contaminants adsorbed (Masliyah et al., 1996), were used as a “reference state” to evaluate mass of bitumen contained in the aggregates. These two relationships were also used to cover a wider range of the aggregate size and to illustrate how a choice of the “reference state” can affect the evaluated mass of solids and air in an aggregate.

Assuming gravity acceleration $g = 981 \text{ cm/s}^2$, viscosity $\mu = 0.01 \text{ g/cm}\cdot\text{s}$, surface tension $\sigma = 60 \text{ mN/m}$, and density $\rho = 1 \text{ g/cm}^3$ of continuous medium, the velocity U of unloaded contaminated bubbles (Clift et al., 1978), can be expressed as a function of bubble diameter and the density difference, $\Delta\rho$, between dispersed and continuous phases:

$$U = 49.29 \Delta\rho^{0.495} d^{0.514} - 0.298 / \Delta\rho^{0.149} d \quad (9)$$

where the bubble diameter d is expressed in cm, and U in cm/s. Equation (9) is valid for bubble diameters d :

$$0.052 \leq d \leq 0.28 \text{ cm} \quad (10)$$

and will be hereafter referred to as Model A.

For the case of non-contaminated freely rising air bubble, its velocity can be expressed as (Masliyah et al., 1994):

$$U = 9.04 \Delta\rho^{0.5} d^{0.5} \left(\frac{Re}{1 + 0.077 Re^{0.65}} \right)^{1/2} \quad (11)$$

where Re is the Reynolds number. Equation (11) is valid for $Re < 130$ and will be used as a second “reference state” and called further as Model B.

The aggregate apparent density was calculated from values of the apparent density difference $\Delta\rho$ between the aggregate and the continuous phase. The apparent density difference $\Delta\rho$, which caused lowering velocity of unloaded air bubble to the measured velocity of the bitumen–air aggregate, was found by solving Eq. (9) (Model A) and Eq. (11) (Model B) in respect to $\Delta\rho$. Next, the mass of bitumen was calculated (Eq.7) using values of the aggregate apparent density obtained on a basis of the both models.

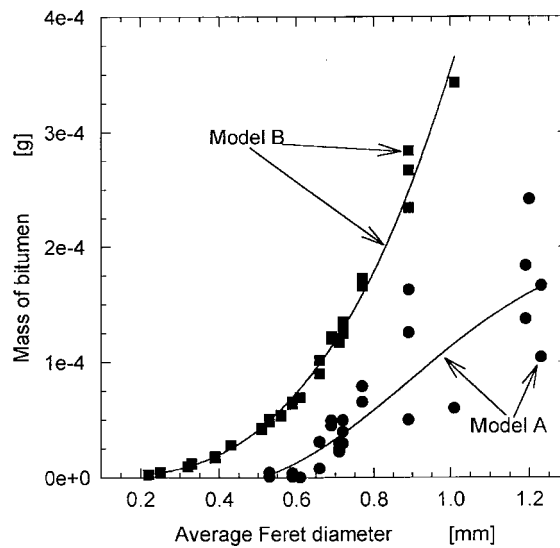


Fig. 10. Comparison of the mass of bitumen in an aggregate calculated on the basis of relationships describing velocity of unloaded contaminated (Model A) and clean (Model B) air bubbles.

Points show the mass of bitumen obtained from the measured individual data points, while lines show the values obtained on the basis of the regression line fitted to the measured velocity data. Rys. 10. Porównanie mas bituminu w agregatach obliczonych na podstawie zależności opisujących prędkości baniek w zanieczyszczonej surfaktantem (Model A) i czystej wodzie (Model B). Punkty pokazują masę bituminu obliczoną na podstawie pojedynczych mierzonych wartości, natomiast linie pokazują wartości uzyskane na podstawie linii regresji dopasowanych do zmierzonych wartości prędkości agregatów

Figure 10 presents the mass of bitumen contained in the bubble-bitumen aggregate as a function of the aggregate average Feret diameter obtained from Models A and B, i.e. for the cases when relationships describing motion of unloaded contaminated and

clean air bubbles were used, respectively, as a “reference state”. Points of Figure 10 show the mass of bitumen calculated from the measured velocity values, while the full line shows the aggregate apparent density calculated on the basis of the regression line fitted to the measured velocity values of the aggregates. It is seen in Fig. 10 how important is the choice of a “reference state”. Absolute values of the mass of bitumen calculated from Model A are lower than those calculated on the basis of Model B because velocity of unloaded air bubbles rising in pure water is higher than in the presence of a surface active contamination (Levich, 1962). However, the both models lead to obtaining a similar order of magnitude of the mass of bitumen contained in an aggregate and the both models show that the mass of bitumen contained in an aggregate increases with increasing aggregate diameter.

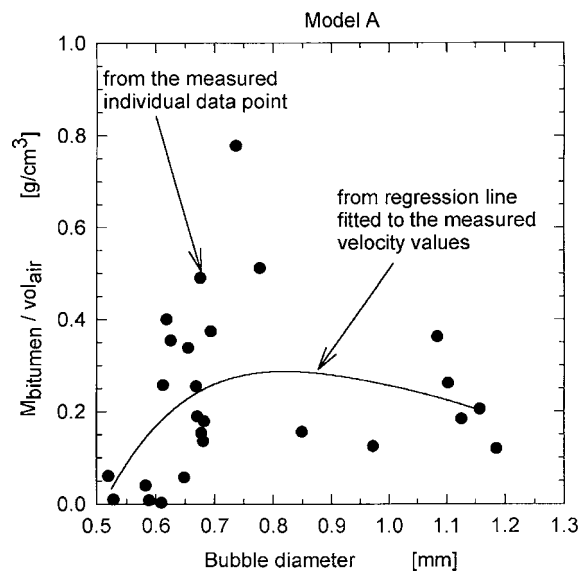


Fig. 11. Dependence of the mass of bitumen per unit volume of air ($M_{\text{bitumen}}/V_{\text{air}}$) on the equivalent diameter of air bubble associated with an aggregate – Model A
 Rys. 11. Zależność masy bituminu na jednostkę objętości powietrza zawartego w agregacie ($M_{\text{bitumen}}/V_{\text{air}}$) od równoważnej średnicy bańki tworzącej agregat bitumin–bańka – Model A

In flotation some surface active contamination are always expected to be present. Therefore, Model A seems to be a more appropriate choice as a “reference state” for evaluation of the mass of solids in floating aggregates. However, Model A cannot be applied for small aggregates. As far as we are aware, there is no available relationship describing motion of unloaded contaminated bubbles as $d \rightarrow 0$. In this situation, applying for small aggregates the relationship describing velocity of unloaded non-contaminated bubble (Model B) seems to be the only reasonable solution. This is also consistent with data presented by Clift et al. (1978) that velocities of bubbles in contaminated and pure water start to be similar at diameters smaller than 0.6 mm.

Collisions, attachment and detachment of grains to bubbles in a separation vessel is a stochastic process. Therefore, bubbles can be loaded to different extend with solids. This can be noticed in Fig. 10 where significant fluctuations in the mass of bitumen determined directly from the measured individual aggregate velocity values can be observed. Using regression line values of the aggregate velocity vs. its dimension leads, as could be expected, to a smooth dependence of the mass of bitumen contained in the aggregate on its average Feret diameter. This is shown by a full lines in Fig.10.

Every aggregate consists of bitumen and air, where the air bubble acts as a carrier. A ratio of mass of bitumen per unit volume of air contained in an aggregate can be a useful information regarding the bubble diameter that is most effective in bitumen transport to the froth layer, i.e. carrying the largest amount of bitumen per unit air volume. Equivalent diameter of an air bubble associated with a bitumen–air aggregate can be obtained using Eq. 4. Figure 11 shows a dependence of the mass of bitumen per unit volume of air ($M_{\text{bitumen}}/V_{\text{air}}$ - calculated on the basis of Model A) on the equivalent diameter of air bubble associated with an aggregate. Here again points show the ($M_{\text{bitumen}}/V_{\text{air}}$) values obtained directly from the measured individual velocity values, while the line was obtained using the aggregate velocity values from the regression line. The ($M_{\text{bitumen}}/V_{\text{air}}$) values fluctuated from zero to almost 0.8 with the mean of 0.20 ± 0.19 g of bitumen being carried by 1 cm^3 of air contained in an aggregate. Data obtained on the basis of the regression line fitted to the measured aggregate velocity values indicate that there seems to be an optimum size range of air bubbles (from ca. 0.65 to 1.1 mm) for which a highest mass of bitumen was transported by a unit volume of air.

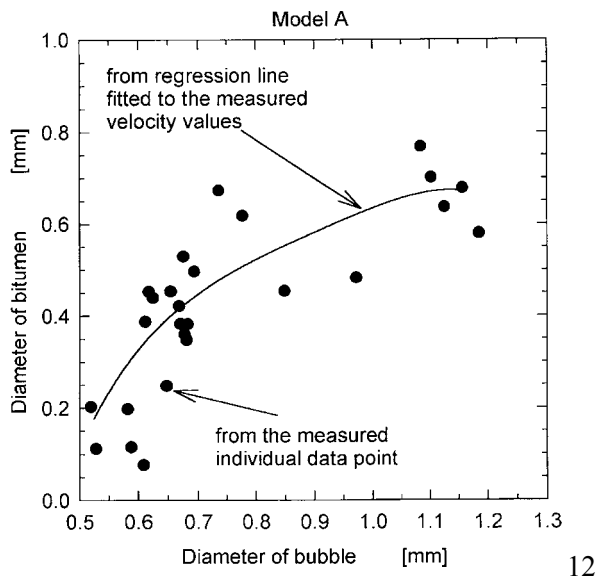


Fig. 12. Equivalent diameter of a bitumen particle as a function of an equivalent diameter of air bubble associated with an aggregate – Model A
Rys. 12. Równoważna średnica cząstki bituminu w funkcji równoważnej średnicy bańki tworzących agregat (bitumin–bańka) – Model A

Finally, an equivalent diameter of bitumen material contained in the aggregate can also be calculated on a basis of the mass of bitumen and its density. Figure 12 presents comparison of equivalent diameters of bitumen particle and air bubble making-up a bitumen–air aggregate. It is seen in Fig. 12 that the equivalent diameter of bitumen contained in an aggregate is smaller but of a similar order of magnitude as the bubble diameter. This is a most striking difference in comparison to metal ores flotation where grain dimensions (Trahar, 1981) are normally many times smaller than the bubble size (Yoon and Lutrell, 1989). However, it should be remembered that bitumen density (1018 kg/m^3) is only slightly higher than water, while density of metal ores is always much higher. Flotation limit for coarse particles (Ralston, 1992) is inversely proportional to the density difference between the particle and water. Due to bitumen low density, larger bitumen particles can be carried out by air bubbles.

CONCLUSIONS

The visualization technique described in this presentation can be easily applied for study of bubble–grain aggregate flow in various mineral flotation cells. Size, shape, rise velocity and number of the aggregates floating to the froth layer at a given location of the separation vessel can be determined using the Luba tube and performing the data analysis presented above. Measurements of the aggregate flux in various areas of a separation vessel can provide information regarding possibility of improving the performance of a flotation cell.

It was found in studies of bubble–bitumen aggregates transport in low energy extraction process of oilsands that the bitumen was transported to the froth layer in a form of irregular entities attached to air bubbles. A wide range of the bitumen–air aggregate sizes (from 0.13 mm to 2.84 mm) was observed with an average Feret diameter, i.e. an equivalent circular diameter of 0.68 ± 0.35 mm. Under steady state flow conditions the average aggregate rise velocity was 6.8 ± 1.8 cm/s with velocities ranging from 3.0 to 12.6 cm/s for individual bubble–bitumen aggregates. The flux of the bitumen–air aggregates was different in various areas of the separation vessel which indicates that performance of the vessel was not the best possible.

A method for the evaluation of mass of solids contained in an air–solids aggregate rising inside a separation vessel to the froth layer was presented. It was shown that the aggregate rise velocity and its dimension were the only experimental data needed to determine the composition of the bitumen–air aggregate. Relationship describing rise

velocity of unloaded air bubble of identical dimensions was used as a “reference state”.

Financial support of NSERC Industrial Research Chair in Oil Sands (University of Alberta) and Syncrude Canada Ltd. is gratefully acknowledged.

REFERENCES

- CLIFT R., GRACE, J.R., WEBER, M.E., 1978, *Bubbles, drops and particles*, New York, San Francisco, London, Academic Press, chap. 9, 221.
- LEVICH V.G., 1962, *Physicochemical hydrodynamics*, Prentice-Hall, Inc., Englewood Cliffs, N.J., chap. VIII, 395.
- MAŁYSA K., NG S., CYMBALISTY L., CZARNECKI J., MASLIYAH J., 1998a, *A method of visualization and characterization of aggregates flow inside a separation vessel. I. Size, shape and rise velocity of the aggregates*, Intern. J. Mineral Process. (to be published).
- MAŁYSA K., NG S., CZARNECKI J., MASLIYAH J., 1998b, *A method of visualization and characterization of aggregates flow inside a separation vessel. II. Composition of the air-bitumen aggregates*, Intern. J. Mineral Process. (to be published).
- MASLIYAH J.H., JAUHARI R., GRAY M.R., 1994, *Drag coefficient for air bubbles rising along an inclined surface*, Chem. Engin. Sci., 49, 1905–1911.
- MASLIYAH J.H., JAUHARI R., GRAY M.R., 1996, *Rise velocities of air bubbles along an inclined surface* [In:] N. Cheremisinoff (Ed.) *Advances in Engin. Fluid Mech.*, Mixed-Flow Hydrodynamics, chap. 25.
- RALSTON J., 1992, *The influence of particle size and contact angle in flotation*, [In:] *Colloid chemistry in mineral processing*, Laskowski, J.S. and Ralston, J. (Eds.), Elsevier, chap. 6, 203.
- RUSS J.C., 1995, *The image processing handbook*, 2nd Edition, CRC Press, Inc., 511.
- SigmaScanPro automated image analysis software. User's manual*, Copyright 1993–1995, Jandel Corporation.
- TRAHAR W.J., 1981, *A rational interpretation of the role of particle size in flotation*, Intern. J. Mineral Process., 8, 289–327.
- YOON R-H., G.H. LUTRELL G.H., 1989, *The effect of bubble size on fine particle flotation*, Mineral Process. Extractive Metall. Review, 5, 101.

Małysa K., Ng S., Czarnecki J., Masliyah J., Metoda pomiaru i analizy rozmiarów, kształtu, prędkości wznoszenia i rozmiarów agregatów flotacyjnych wpływających do warstwy piany. *Fizykochemiczne Problemy Mineralurgii*, 32, 91–108 (w jęz. angielskim)

Przedstawiono metodę pomiaru i analizy rozmiarów, kształtu oraz prędkości wznoszenia i składu agregatów flotacyjnych bańka–ziarna wpływających wewnątrz komory flotacyjnej do warstwy piany. Strumień agregatów bańka–ziarno płynących wewnątrz komory flotacyjnej był monitorowany przy pomocy urządzenia nazwanego *Luba tube*. Zasada działania aparatu Luby polega na wyprowadzeniu powyżej warstwy piany strumienia agregatów płynących do tej warstwy piany. Kiedy cylinder napełniony wodą jest szczelnie przykryty, obrócony i zanurzony do szerszego pojemnika z wodą, wtedy także po usunięciu tego szczelnego przykrycia słup wody w cylindrze może być znacznie powyżej poziomu cieczy w szerokim pojemniku. Jeżeli pod ten otwarty koniec cylindra napłyną bańki lub agregaty flotacyjne to będą one wypływać do góry wewnątrz cylindra i ich przepływ może być obserwowany i rejestrowany powyżej brzegów szerokiego pojemnika (komory flotacyjnej) wypełnionego cieczą (pulpą). Wykonano badania agregatów bańka–bitumin wpływających do warstwy piany

wewnątrz komory flotacyjnej o średnicy 5,2 m używanej w pilotowej instalacji (100 ton/godz.) do opracowania niskoenergetycznego procesu przeróbki piasków roponośnych. Wyznaczono rozmiary, kształt oraz prędkości wznoszenia i zawartości części stałych w agregatach bańka-bitumin wypływających do warstwy piany oraz strumienie agregatów w różnych punktach komory flotacyjnej. Stwierdzono, że bitumin był transportowany do warstwy piany w postaci nieregularnych cząstek przyczepionych do baniek. Rozmiary agregatów bańka-bitumin były w zakresie od 0,13 do 2,84 mm, przy czym wartość średnia średnicy Fereta, tj. równoważnej średnicy kołowej, wynosiła $0,68 \pm 0,35$ mm. W warunkach stanu stacjonarnego średnia prędkość wznoszenia agregatów bańka-bitumin wynosiła $6,8 \pm 1,8$ cm/s, przy czym obserwowano prędkości agregatów od 3,0 do 12,6 cm/s. Obliczono masy bituminu zawartego w agregatach bańka-bitumin w oparciu o wyznaczone rozmiary i prędkości ich wypływania oraz używając literaturowe zależności opisujące prędkości baniek w zanieczyszczonej surfaktantem (Model A) i czystej wodzie (Model B). Masa bituminu zawarta w badanych agregatach była rzędu od 10^{-6} do 10^{-4} g w zależności od rozmiarów agregatu. Wyznaczone równoważne średnice cząstek bituminu i baniek gazowych tworzących agregaty były podobnej wielkości w zakresie 0,2–1,2 mm. Strumień agregatów płynących do warstwy piany był różny w różnych punktach komory flotacyjnej. Najwięcej agregatów wypływało do warstwy piany w pobliżu środka (lokalizacja 1 – $r = 0,9$ m), a najmniej w pobliżu ścian (lokalizacja 3 – $r = 2,3$ m) komory flotacyjnej. Stosunek liczby agregatów płynących do warstwy piany w lokalizacjach 1 i 3 wynosił 4,1 : 1. A zatem nie cała powierzchnia badanej komory flotacyjnej była wykorzystana równie efektywnie, co najprawdopodobniej było związane z nierównomiernym rozłożeniem nadawy w komorze.